



Corrosion resistance and hydrophilic properties of plasma sprayed Ni+5% Al coatings



Mojtaba Rezaee Hajideh^a, Mohammadreza Farahani^{a,*}, Mohammadjavad Pakravan^b, Ali Shahmirzalo^a

^a School of Mechanical Engineering, College of Engineering, University of Tehran, Iran

^b School of Mechanical Engineering, Aborz Campus, University of Tehran, Iran

ARTICLE INFO

Keywords:

Mechanical engineering
Nickel aluminum powder
Plasma spraying
Potentiodynamic measurement
Corrosion resistance
Contact angle

ABSTRACT

In this research, the AZ31 Mg alloy was coated with Ni5Al powder, using a plasma spray method. Effects of nozzle distance and number of passes on corrosion behavior, hydrophilic properties and phase structure of the coated layer were studied. Samples in different distance of nozzle (150 and 300 mm) and different number of passes (2, 4 and 6) were examined. Corrosion behavior characterization was carried out using electrochemical impedance spectroscopy and potentiodynamic polarization methods. Hydrophilic properties of the coated layer were also investigated by the contact angle method. Results showed that by increasing the number of passes, the corrosion resistance and the contact angle were increased. On the other side, by increasing the nozzle distance, the corrosion resistance and the contact angle were decreased. The Coated sample with 6 pass coating and nozzle distance of 150 mm had the best corrosion behavior and hydrophilic properties.

1. Introduction

Due to low density and, high strength of magnesium alloys, they are suitable materials for low-weight industrial applications such as automotive and aerospace industries [1]. However, the low corrosion resistance of magnesium and its alloys, especially in chlorinated environments, is its major drawback. Creating protective metal or ceramic coatings on the magnesium alloy surface using plasma spray technique is one alternative to increase their corrosion resistance. Plasma spray is a complex and basic method for hot spraying [2, 3, 4, 5]. In this method, with the aid of a DC voltage, high temperature plasma gas is produced which act as a heat source during the spraying of the powders. The powder is injected into the nozzle and then melted and thrown onto the sample surface with the aid of plasma gas. Various factors affect the adhesion strength, mechanical properties and the corrosion resistance of the coating layer produced by the plasma spray method [3, 4, 5, 6, 7]. Nozzle distance from the substrate, coating pass number, applied spark current, preheating temperature [8], substrate preparation [6, 7, 8, 9] and percentage of aluminum and nickel in powdered alloys [10] are the effective parameters on the metal spray coating process. Moridi et al. and Sattari et al. [11, 12] have examined the effect of pass number on the thickness and mechanical properties of aluminum coatings using spray

coating method. They observed the hardness of the coating layer was not affected by changing the number of passes, but the residual stresses were increase by increasing the number of passes. Kubatick et al. [10, 15] examined the effect of preheat temperature on the metallurgical bands of nickel-aluminum coat on the magnesium substrate. They observed that by increasing the pre-heat temperature, the metallurgical bands improved and the adhesive strength increased. Li et al., Kozerski et al. and Kubatík et al. [13, 14, 15] examine the effect of substrate preparation on the adhesion properties of the aluminum-nickel alloy coating on the magnesium-aluminum alloy substrate. They found that the sample preparation, using different methods was effective in adhesion strength of the coating layer. Jiří Matějčíček et al. [8] investigated the effect of preheating temperature and distance from the nozzle on the properties of the tungsten coating layer by plasma spray method. They observed that, at lower distances and at higher preheating temperature, the grains grow in columnar form. Also, by increasing the preheating temperature, the hardness of the coating layer increased. Behnoosh Sattari et al [11] examined the effect of pass number of the plasma spraying on the corrosion properties of iron-aluminum alloy coating on steel substrate. They observed that by increasing the number of passes, the polarization resistance and the impedance of the formed layer increased and its corrosion properties improved [15, 16, 17, 18, 19].

* Corresponding author.

E-mail address: mrfarahani@ut.ac.ir (M. Farahani).

<https://doi.org/10.1016/j.heliyon.2019.e01920>

Received 27 December 2018; Received in revised form 10 May 2019; Accepted 4 June 2019

2405-8440/© 2019 Published by Elsevier Ltd. This is an open access article under the CC BY-NC-ND license (<http://creativecommons.org/licenses/by-nc-nd/4.0/>).

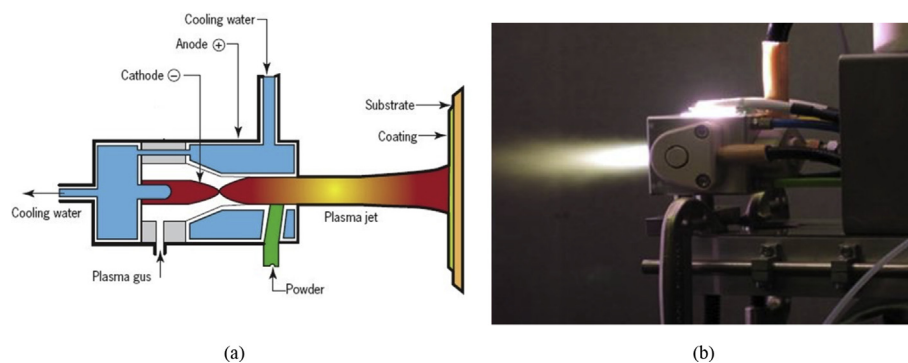


Fig. 1. (a) Schematics of plasma spray process and (b) The employed plasma spray device.

Table 1

Plasma spray process condition for the prepared samples.

Sample code	Nozzle distance (mm)	Number of pass
2P-150	150	2
4P-150	150	4
6P-150	150	6
2P-300	300	2
4P-300	300	4
6P-300	300	6

In this research, AZ31 magnesium alloy was used as substrate. Magnesium and its alloys are the engineering materials which have the potential ability to be used widely in the automotive, in the aerospace and in the biomedical sectors [20, 21]. However, due to their poor wear resistance and corrosion resistance, their usage is being restricted. This situation prevents Mg alloys to be used without any surface protection despite their good mechanical properties. In this study, plasma spraying method is used to improve the corrosion resistance of AZ31 Mg alloy [22, 23].

The Ni5Al generated coatings in high temperature have diffusion with metal substrate [24]. In addition, during deposition process, some participates in coating layer generate. Participates effect on structure, corrosion and wear behavior. Actually, some results showed presence of participates can improve corrosion and wear behavior [25, 26].

The effect of pass number and the distance from the nozzle on the corrosion properties and hydrophobicity of the coating layer created by the plasma spray method has been studied less. In this research, the corrosion resistance, hydrophobicity and phase structure of the Ni5Al coating layer on the AZ31 substrate were examined by changing the number of passes from 2 to 6 passes and the nozzle distance from 150 mm to 300 mm.

2. Experimental

2.1. Specimen preparation

In this study, AZ31 magnesium alloy sheet (Al 3.0%, Zn 1.2%, Mn 0.2%, balance Mg) was cut into rectangular samples of 30 mm × 20 mm × 5 mm dimensions as the substrates to be coated. Samples were coated using a plasma spray method. The Ni5Al (wt %) powder (provided by the Metco company), with particle size of 45–90 μm, was used as a feedstock material [27]. Ni5Al coatings are dense and resistant to oxidation and abrasion, recommended for use as oxidation-resistant bond coats which can be used up to 800 °C (1470 F). Self-bonding and undergoes an exothermic reaction during spraying, resulting in excellent bonding to the substrate [28]. Before the coating process, samples cleaned by sandblasting. The plasma spray process performed by a WSP-H500 plasma spray device. The employed device and the schematics of plasma spray process are presented in Fig. 1. The applied voltage was

500V and the established current was 400A. Different nozzle distance from 100 to 400 mm were considered for the primary examinations. Small nozzle distance led to substrate melting while the separation of the coated layer from the substrate was observed at large nozzle distance. Consequently, the nozzle distance of 150 and 300 mm were considered as the appropriate distances in this study. Different spraying pass numbers were usually employed for different application. In this study the effect of pass number was also considered. So, in each nozzle distance, samples were sprayed at 2, 4 and 6 passes. The plasma spray process conditions of the prepared samples are reported in Table 1.

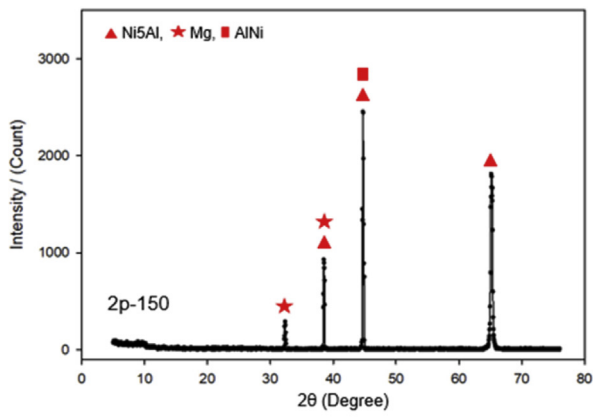
2.2. Characterization of the coated layer

The corrosion behavior of the coated layer was analyzed with electrochemical methods. For this purpose, electrochemical impedance spectroscopy (EIS) and potentiodynamic polarization tests were conducted according to ASTM G102-98-E1 and ASTM B457-67 standards, respectively [29]. The EIS and potentiodynamic polarization tests were carried out with EG&G-VersaSTAT4 potentiodynamic device. These tests were conducted on a circle area with 5 mm diameter on the surface of the sample and in %3.5 NaCl solution at room temperature. For electrochemical analysis, three electrodes were used: saturated calomel electrode (SCE), counter electrode and the samples [30]. The samples were initially immersed for 5 minutes in the solution of %3.5NaCl to reach a stable open circuit potential (OCP). Potentiodynamic test was carried out in the potential range of -500 mV below OCP potential and +800 mV above OCP with a scan rate of 1 mV/s. Also, EIS test was carried out in a frequency range of 0.01 to 10⁵ Hz with a +30mV amplitude voltage with respect to OCP. The experimental data from EIS test was fitted using ZSimpWin 3.21 software and the suitable equivalent EIS circuit parameters were extracted. In order to characterize the corrosion surface. After potentiodynamic polarization test, the specimens were examined using JSM-7610F scanning electron microscope. The properties of the coated samples were also measured with x-ray diffraction (XRD) Panalytical, with Cu Kα x-ray ($\lambda = 1.5418\text{\AA}$) and with an incident angle of $w = 1^\circ$. The surface Hydrophobic properties of the coated samples were characterized using contact angle method. These analyses were conducted at room temperature and in distilled water and the needle diameter 0.793 mm. The contact angle measurement was carried out on 5 different points. The average result was reported in the following. The measurement had 2^o tolerance.

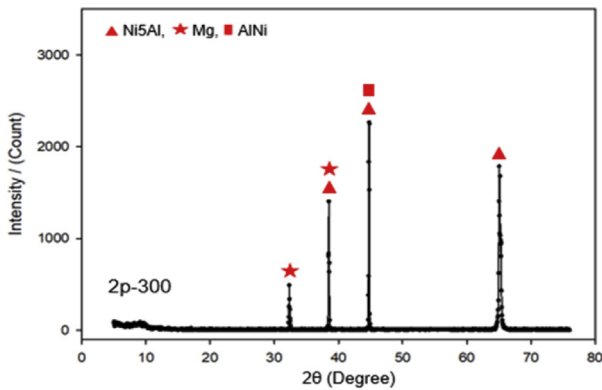
3. Results and discussion

3.1. X-ray pattern study

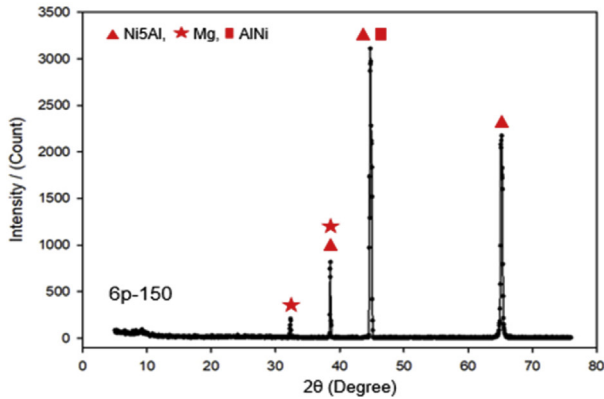
Fig. 2 shows the X-Ray pattern of Ni5Al layer, deposited on the AZ31 alloy substrate. As it can be seen in X-Ray pattern, Ni5Al and probably NiAl deposited layer were obtained. X-Ray pattern indicates that by increasing the nozzle distance from 150 to 300 mm in two passes



(a)



(b)



(c)

Fig. 2. The XRD pattern of the generated phases in Ni5Al layer: a) 2P-150, b) 2P-300 and c) 6P-150.

samples, the intensity of Ni5Al peaks was decreased. Actually, by increasing the nozzle distance, the thickness of the coating layer was decreased. Fig. 2 (c) shows the X-Ray pattern of 6P-150 sample. By increasing the number of passes of plasma spraying, the intensity of Ni5Al and probably NiAl, on the deposited layer was increased. The thickness of deposited layer in 6 passes sample was also higher than the 2 and 4 passes samples.

3.2. Potentiodynamic polarization analysis

Fig. 3 presents potentiodynamic polarization curves for the samples

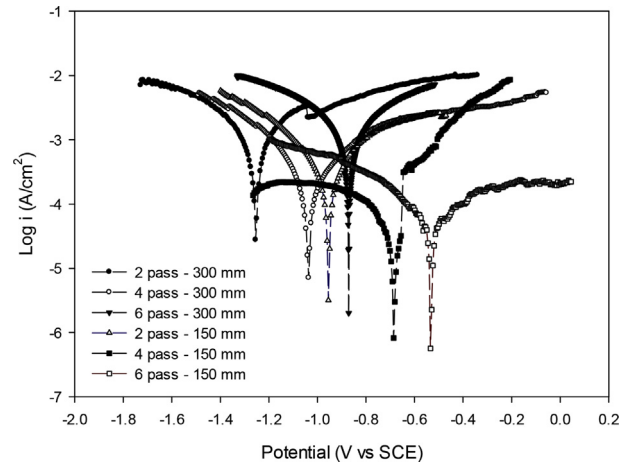


Fig. 3. Potentiodynamic polarization curves of the coated samples.

Table 2

Potentiodynamic polarization test results.

Sample	I _{corr} (μA)	E _{corr} (mV)	-β _a (mV)	β _c (mV)	R _p
2p-150	49.811	-943.2	166.208	178.035	749.329
4p-150	12.589	-687.3	68.36	61.99	1121.314
6p-150	6.309	-523.7	59.646	51.118	1894.532
2p-300	94.361	-1257.8	124.244	146.272	309.142
4p-300	50.11	-1073.9	116.665	108.48	487.091
6p-300	39.367	-861.3	204.244	146.272	940.105

prepared at different distances of nozzle and number of passes. E_{corr} and I_{corr} values, the tangent line in the linear region on the anodic and cathodic branches of the potentiodynamic polarization curves are reported in Table 2. The value of potentiodynamic polarization resistance was calculated with Versa-stat software with respect to the following equation:

$$R_p = \frac{1}{2.303 \left(\frac{1}{\beta_a} + \frac{1}{\beta_c} \right) i_{Corr}} \quad (1)$$

In this equation, R_p is the polarization resistance, β_a, is the slope of anodic branch and β_c, is the slope of cathodic branch. As it could be seen in Table 2, in 2- pass-coated sample, by increasing the nozzle distance from 150 mm to 300 mm, corrosion resistance R_p was decreased from 749.329 to 309.142 Ω/cm². Increased corrosion current and decreased corrosion potential were due to decreasing the corrosion resistance. It can be mentioned that by increasing the nozzle distance, the porosity of coating layer increased and its homogeneity decreased. The porosity in the coating layer acted as preferred corrosion location. In other words, in low distances of nozzle, particles in coating layer were dense and created a uniform surface. In this situation, the penetration of the corrosive solution was decreased which resulted in better corrosion behavior. In the same nozzle distance, by increasing the number of passes, thickness of Ni5Al layer and the uniformity of Ni5Al layer were increased. Therefore, the 6-pass sample with a distance of 150 mm of nozzle, had a lower corrosion rate and its polarization resistance was 1894.532 Ω/cm² which was higher than all the other samples.

3.3. Electrochemical impedance spectroscopy (EIS) analysis

Fig. 4 presents the experimental and fitted Nyquist, bode and bode phase diagrams for 2P-150, 4P-150, 6P-150, 2P-300, 4P-300 and 6P-300 samples. Equivalent circuit proved for coated AZ31 substrate was LR (C (R (QR))) (CR), consisting of capacitance loops and an inductive loop in high frequencies.

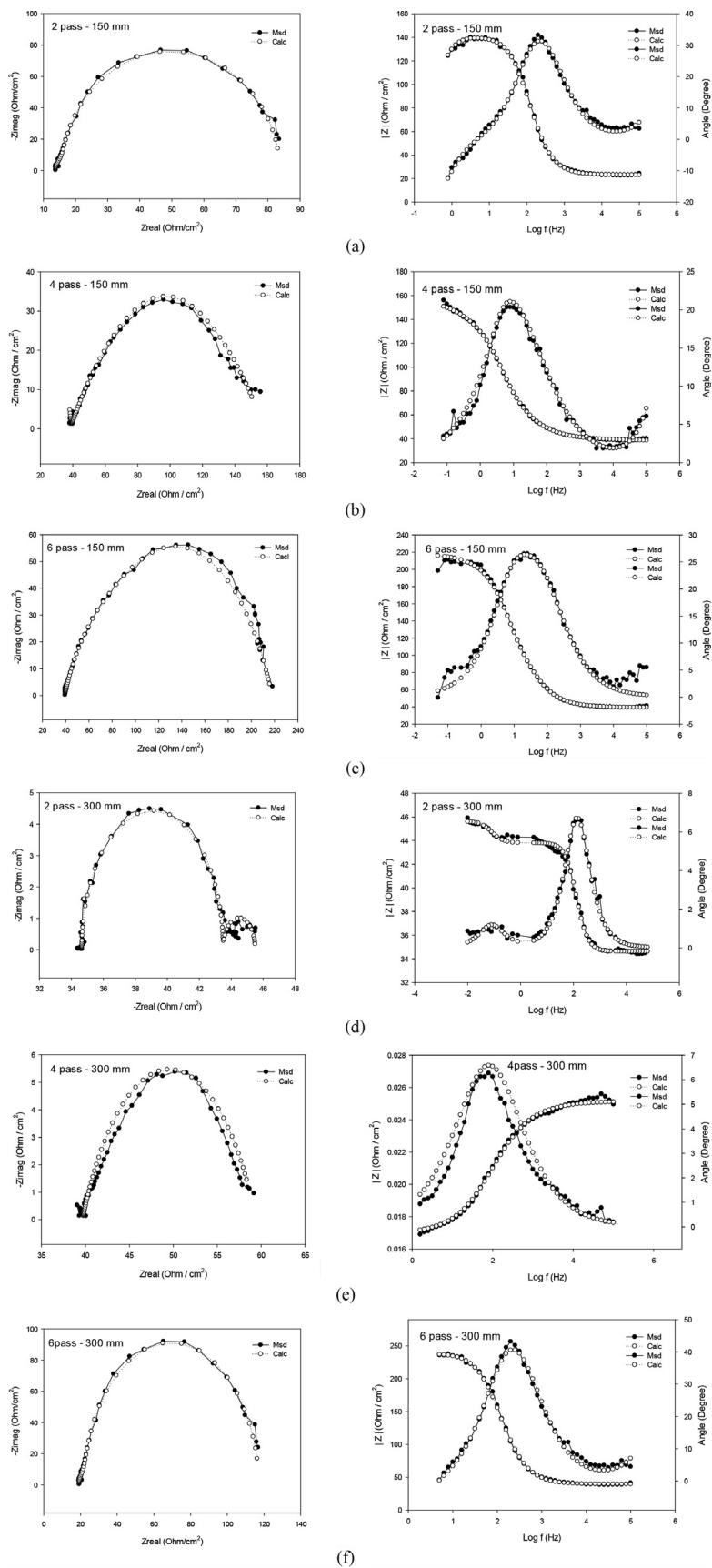
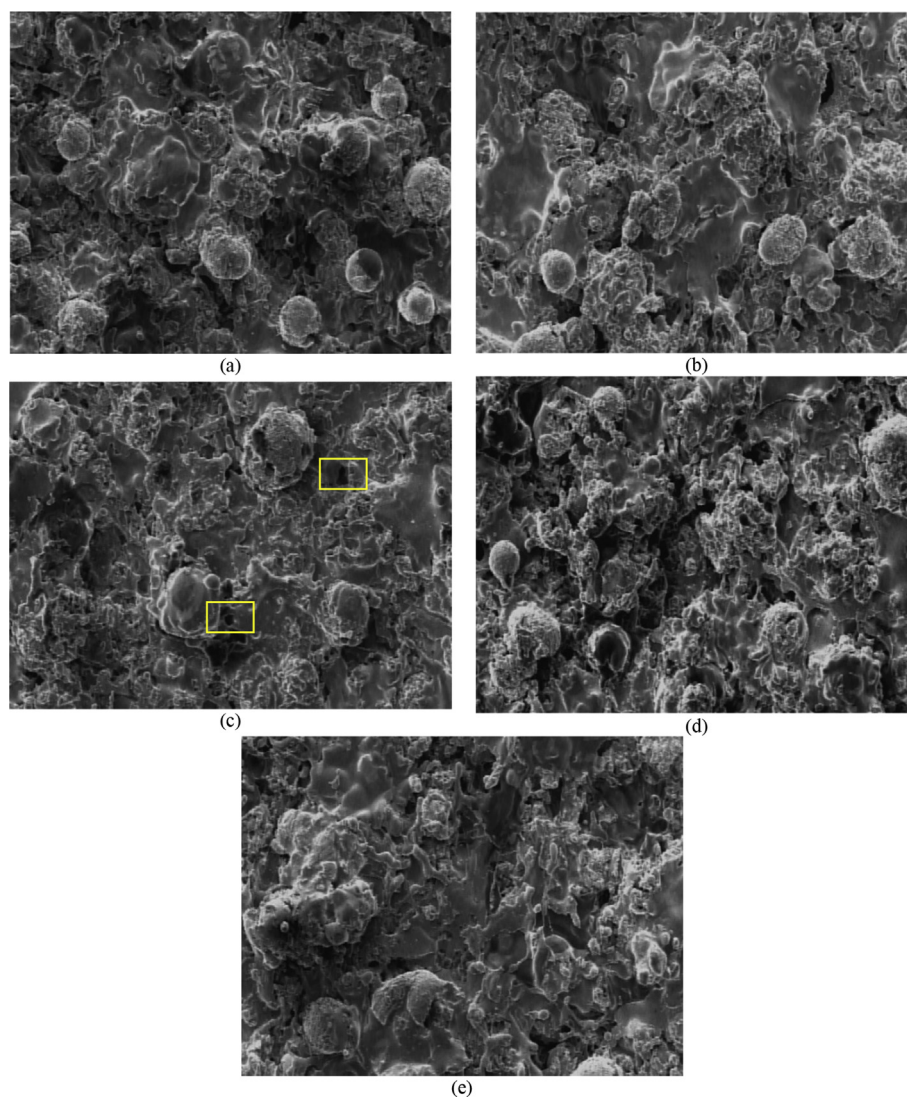


Fig. 4. Nyquist, bode and bode-phase diagrams of the coated specimen in 3.5% wt NaCl solution, a)2P-150, b)4P-150, c)6P-150, d)2P-300, e)4P-300, f)6P-300.

Table 3

Electrochemical parameters of EIS for the coated specimens.

Sample	L1	R1	C2	R2	Q3-Y0	Q3-m	R3	C4	R4	K square
2p-150	2.055E-13	34.76	0.00363	27.49	0.006393	0.6206	32.33	0.004478	64.21	2.489E-4
4p-150	1.89E-13	34.61	0.001387	91.91	0.0013	0.744	104.51	0.002785	149.7	5.56E-4
6p-150	1.37E-13	35.22	0.000781	112.48	0.0003317	0.8	137.4	0.0003274	412.6	1.373E-4
2p-300	2.83E-13	35.97	0.006791	10.27	0.008931	0.4778	13.61	0.009664	16.37	2.614E-4
4p-300	2.215E-13	34.7	0.00484	15.66	0.007706	0.5726	14.69	0.007108	19.41	3.84E-4
6p-300	1.98E-13	35.58	0.00203	47.77	0.002462	0.6991	54.93	0.005986	93.56	3.091E-4

**Fig. 5.** Images of corroded surface in a) 2P-150, b) 4P-150, c) 6P-150, d) 2P-300 and e) 4P-300 samples.

In the equivalent circuit, R_{sol} is the resistive behavior of solution, R_s , the electrical resistance of the surface coating, R_{dl} , electrical resistance behavior of the double electrical layer, L , pitting corrosion behavior of open pores and eventually, R_p , the electrical resistance behavior of the generated pits. In addition, three constant phase elements (CPE) exist which are CPE_s , CPE_p and CPE_{dl} . These stand for the dielectric characteristics of surface coating, the generated pits and the double electrical layer, respectively. In other words, this parameter shows the deviation from ideal capacitive behavior and decreasing uniformity of the surface. The value of CPE can be calculated from EIS spectra at lower frequencies about 0.01–1 Hz. For this purpose, Eq. (2) can be used.

$$Z_{CPE} = (Q(j\omega)^\alpha)^{-1} \quad (2)$$

Where Q , j , ω and α are all derived from the ZSimpWin 3.21 software. Electrochemical EIS parameters values were obtained by ZSimpWin 3.21 software and are reported in Table 3. By increasing the number of passes for the nozzle placed at a distance of 150 mm, the diameter of capacitance loop in Nyquist diagram was increased. Consequently, it could be noted that by increasing the number of passes in the same nozzle distance, the corrosion resistance was increased. It can be explained as by increasing the number of passes, thickness and uniformity of Ni5Al layer were increased and the porosity generated in Ni5Al layer was decreased. The bode impedance diagrams slope presents the surface homogeneity. The slope close to 1, indicates the increase in corrosion resistance. The lower slope, shows the decrease in corrosion resistance. By increasing the pass number, the slope of the linear part of bode diagram for the samples

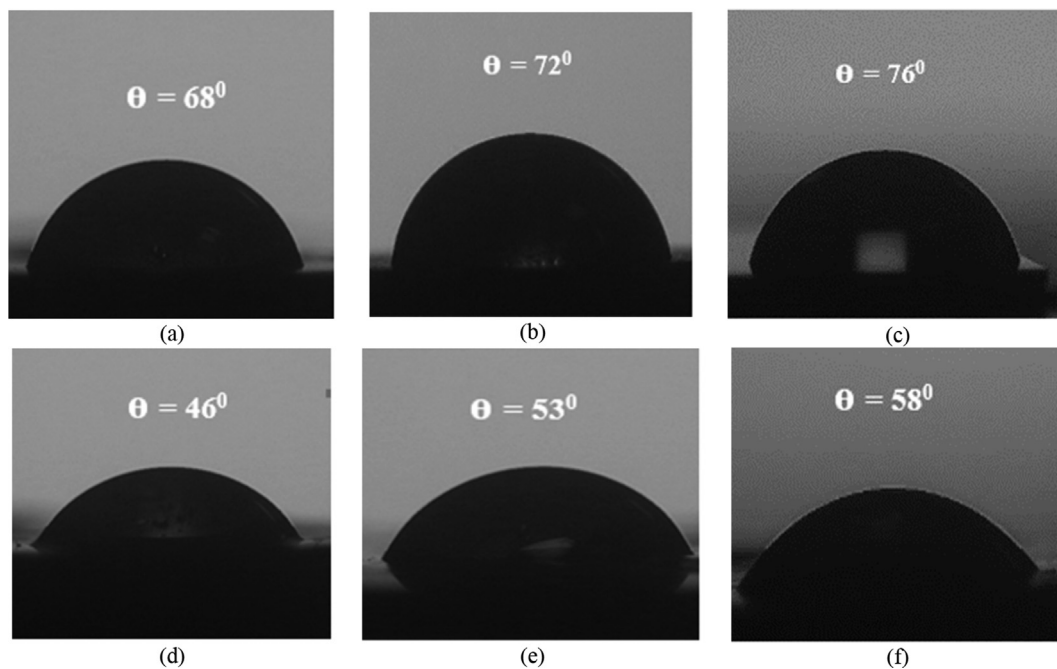


Fig. 6. The contact angle images of Ni5Al layer in a) 2P-150, b) 4P-150, c) 6P-150, d) 2P-300, e) 4P-300 and f) 6P-300 samples.

with 150 mm nozzle distance was increased and approached to 1. The bode diagrams presents that by increasing the number of passes, the corrosion resistance increases. The 6P-150 sample has the highest slope of linear part of bode diagram as its surface is homogenous with minimum surface porosity. Fig. 4 shows experimental and fitted Nyquist, bode and bode phase diagrams for 4P-300 sample. Comparison between 4P-150 and 4P-300 samples shows that the diameter of Nyquist diagram for 4P-300 sample was decreased; it shows that the corrosion resistance was decreased by increasing the nozzle distance. By increasing the nozzle distance, the thickness of Ni5Al layer and its surface homogeneity were decreased and its surface porosity was increased. consequently, in 4P-300 sample, the slope of the linear part of bode diagram was decreased in comparison to 4P-150 sample.

3.4. SEM morphology of the corroded surface

Fig. 5 shows the image of the corroded surface of 2P-150, 4P-150, 6P-150, 2P-300 and 4P-300 samples after potentiodynamic polarization test in the solution of 3.5 % wt. NaCl at room temperature [31]. Fig. 4(a), (b) and (c) show the corroded area of the coated samples in a same nozzle distance with different number of passes. It was observed that by increasing the number of passes, the corroded area was decreased. In the deposited layer, the mechanism of corrosion is pitting. Density of created pits and pit effective area were decreased by increasing the number of passes. In this case, in 6P-150 sample, the coated layer was dense and the bond between Ni5Al particles was stronger. It can be explained that by increasing the number of passes, the porosity of Ni5Al layer was decreased. Therefore, the number ready locations for corrosion were decreased. Fig. 4 (d) and (e), shows that by increasing the nozzle distance, density of pits and their effective area were increased. By increasing the nozzle distance, the thickness of Ni5Al was decreased, the bond between the particles were weaker, then the porosity of surface was increased. Porosities acted as the preferred corrosion locations and decreased corrosion resistance. Actually, density of pores affected on uniformity of surface and by increasing density of pores, uniformity of surface decreased.

3.5. Contact angle of the coated surface

Fig. 6 shows the contact angle of water drop. Contact angle measurement was performed to determine the water-repellency property of the coated layer in various process condition [32]. In order to measure the contact angle, distilled water with a needle of 0.793 mm diameter at a distance of 2.5 cm from the sample surface were used. As it can be seen, the contact angle changed with changing the number of passes, and the 6-passed sample with a distance of 150 mm had the greatest contact angle. Materials with a contact angle of 0–90° are considered as water-loving material. In water-loving materials, the surface is more water-friendly with increasing the surface roughness and decreasing the contact angle. But at the hydrophobia surface, with increasing the surface roughness, hydrophobicity and the contact angle of the surface will increase. As a result, it can be said that the surface of the Ni5Al coating layer has a hydrophilic property and with decreasing the surface roughness from 2 to 6 passes, the amount of surface hydrophobicity and the contact angle of the coating layer has been increased. As it is mentioned, the coated layer in 6-passed sample had the best corrosion behavior. Surface hydrophobicity was one of the effective factors in corrosion behavior. It can be said that, in addition to lower porosity and uniformity of the coated surface in 6-passed sample, the lower surface roughness and consequently, its better hydrophobicity was also effective in the better corrosion resistance of this specimen.

4. Conclusions

The Ni5Al coating layer was deposited on AZ31 substrate using plasma spray. The corrosion behaviors of the Ni5Al coated layer were investigated using potentiodynamic polarization method, EIS, SEM, CA and XRD measurements. The obtained results could be summarized as follows:

1. In the same nozzle distance, by increasing the number of passes, the corrosion resistance was increased as the 6P-150 sample has the best corrosion behavior.

- By increasing the nozzle distance, localized corrosion was increased and the corrosion resistance was decreased.
- The SEM observations manifested that by increasing the nozzle distance and decreasing the number of passes in plasma spray method, the density of pits and their size were increased.
- The CA tests show that the coated layer in 6-passed sample had the largest contact angle.
- By increasing the number of passes in plasma spray and decreasing the nozzle distance, Ni5Al layer and the intensity of its peak in the XRD pattern were both increased.

Declarations

Author contribution statement

Mohammadreza Farahani: Conceived and designed the experiments; Wrote the paper.

Mojtaba Rezaee Hajideh: Performed the experiments; Wrote the paper.

Mohammadjavad Pakravan, Ali Shahmirzaloo: Analyzed and interpreted the data; Contributed reagents, materials, analysis tools or data.

Funding statement

This research did not receive any specific grant from funding agencies in the public, commercial, or not-for-profit sectors.

Competing interest statement

The authors declare no conflict of interest.

Additional information

No additional information is available for this paper.

References

- Tabasi, M. Farahani, M.K. Besharati Givi, M. Farzami, A. Moharami, Dissimilar friction stir welding of 7075 aluminum alloy to AZ31 magnesium alloy using SiC nanoparticles, *Int. J. Adv. Manuf. Technol.* 86 (2016) 705–715.
- Amin, H. Panchal, A review on thermal spray coating processes, *Int. J. Curr. Trends. Eng. Res* 2 (2016) 556–563.
- J.K. Xiao, W. Zhang, L.M. Liu, X.P. Gan, K. Ch. Zhou, Ch. Zhang, Microstructure and tribological properties of plasma sprayed Cu-15Ni-8Sn coating, *Surf. Coating Technol.* 337 (2018) 159–167.
- M.H. Mathabatha, A.P.I. Popoola, O.P. Oladipo, Residual stresses and corrosion performance of plasma sprayed zinc-based alloy coating on mild steel substrate, *Surf. Coating Technol.* 318 (2017) 293–298.
- O.P. Oladipo, M.H. Mathabatha, A.P.I. Popoola, T.P. Ntsoane, Characterization and corrosion behaviour of plasma sprayed Zn-Sn alloy coating on mild steel, *Surf. Coating Technol.* (2017).
- S. Mahade, N. Curry, S. Björklund, N. Markocsan, P. Nylén, Engineered thermal barrier coatings deposited by suspension plasma spray, *Mater. Lett.* 29 (2017) 517–521.
- K.M. Deen, M. Afzal, Y. Liu, A. Farooq, A. Ahmad, E. Asselin, Improved corrosion resistance of air plasma sprayed WC-12%Co cermet coating by laser re-melting process, *Mater. Lett.* 191 (2017) 34–37.
- J. Matejíček, M. Vilémová, B. Nevrlá, L. Kocmanová, J. Veverka, M. Halasová, H. Hadraba, The influence of substrate temperature and spraying distance on the properties of plasma sprayed tungsten and steel coatings deposited in a shrouding chamber, *Surf. Coating Technol.* 318 (2017) 217–223.
- J. Sun, J. Wang, Sh. Dong, Y. Hui, L. Li, L. Deng, J. Jiang, X. Zhou, X. Cao, Effect of heat treatment on microstructure and property of plasma-sprayed lanthanum hexa aluminate coating, *J. Alloy. Comp.* 739 (2018) 856–865.
- T.F. Kubatík, F. Lukáč, J. Stoužil, P. Čtíbor, F. Půša, K. Stehlíková, Preparation and properties of plasma sprayed NiAl10 and NiAl40 coatings on AZ91 substrate, *Surf. Coating Technol.* 319 (2017) 145–154.
- B. Sattari, M. Shamanian, A. Ashrafi, M. Salehi, F. Salimijazi, Effect of number of passes on the corrosion behavior of Fe/Al surface composites produced by plasma spraying and friction stir processing, *J. Mater. Process. Technol.* 250 (2017) 35–44.
- A. Moridi, S.M. Hassani Gangaraj, S. Vezzu, M. Guagliano, (Number of Passes and thickness effect on mechanical characteristics of cold Spray coating), *Procedia. Eng.* 74 (2014) 449–459.
- J. Li, Ch. X. Li, G.J. Yang, Ch. J. Li, Effect of vapor deposition in shrouded plasma spraying on morphology and wettability of the metallic Ni20Cr coating surface, *J. Alloy. Comp.* 735 (2018) 430–440.
- P. Białucki, S. Zozerski, Study of adhesion of different plasma-sprayed coatings to aluminium, *Surf. Coating Technol.* 201 (2006) 2061–2064.
- T.F. Kubatík, Z. Pala, K. Neufuss, M. Vilémová, R. Mušálek, J. Stoužil, P. Šlepička, T. Chráška, Metallurgical bond between magnesium AZ91 alloy and aluminium plasma sprayed coating, *Surf. Coating Technol.* 282 (2015) 163–170.
- H. FekiGhorbel, A. Guidara, Y. Danlos, J. Bouaziz, Ch. Coddet, Synthesis and characterization of alumina-fluorapatite coatings deposited by atmospheric plasma spraying, *Mater. Lett.* 185 (2016) 268–271.
- F. Einkhah, K.M. Lee, M.A. Faghihi Sani, B. Yoo, D.H. Shin, Structure and corrosion behavior of oxide layer with Zr compounds on AZ31 Mg alloy processed by two-step plasma electrolytic oxidation, *Surf. Coating Technol.* 238 (2014) 75–79.
- V. Deodeshmukh, B. Gleeson, Evaluation of the hot corrosion resistance of commercial β -NiAl and developmental γ -Ni3Al+ γ -Ni-based coatings, *Surf. Coating Technol.* 202 (2007) 643–647.
- Q. Mao, Q. Yang, W. Xiong, Sh. Li, M. Zhang, L. Ruan, Corrosion behavior of Ni3Al-bonded TiC-based cermets in H2SO4 and NaOH solutions, *Ceram. Int.* 44 (2018) 13303–13312.
- M. Farahani, I. Sattari-Far, D. Akbari, R. Alderliesten, Effect of residual stresses on crack behaviour in single edge bending specimens, *Fatigue Fract. Eng. Mater. Struct.* 36 (2013) 115–126.
- M. Farahani, I. Sattari-Far, Effects of residual stresses on crack-tip constraints, *Sci. Iran.* 18 (2011) 1267–1276.
- L. Wu, Yue-hui. He, Y. Jiang, Y. Zeng, Yi-feng. Xiao, B. Nan, Effect of pore structures on corrosion resistance of porous Ni3Al intermetallics, *Trans. Nonferrous Metals Soc. China* 24 (2014) 3509–3516.
- İ. Çelik, Structure and surface properties of Al2O3–TiO2 ceramic coated AZ31 magnesium alloy, *Ceram. Int.* 42 (2016) 13659–13663.
- H. Mohammadzadeh Jamalian, M. Farahani, M.K. Besharati Givi, M. Aghaei Vafaei, Study on the effects of friction stir welding process parameters on the microstructure and mechanical properties of 5086-H34 aluminum welded joints, *Int. J. Adv. Manuf. Technol.* 83 (2016) 611–621.
- L. Du, W. Zhang, W. Liu, J. Zhang, Preparation and characterization of plasma sprayed Ni3Al–hBN composite coating, *Surf. Coating Technol.* 205 (2010) 2419–2424.
- H. Singh, S. Prakash, D. Puri, Some observations on the high temperature oxidation behaviour of plasma sprayed Ni3Al coatings, *Mater. Sci. Eng. A* 444 (2007) 242–250.
- H. Andalib, M. Farahani, M. Enami, Study on the new friction stir spot weld joint reinforcement technique on 5754 aluminum alloy, *Proc. Inst. Mech. Eng., Part C* 232 (2018) 2976–2986.
- P. Ghabezi, M. Farahani, Experimental investigation of nanoparticles effects on cohesive model and bridging laws of mode I fracture in the adhesive joints, *J. Adhes. Sci. Technol.* 31 (2017) 1807–1823.
- P. La, Q. Xue, W. Liu, Sh. Yang, Tribological properties of Ni Al–Cr C composite coatings under liquid 3 7 3paraffin lubrication, *Wear* 240 (2000) 1–8.
- M. Enami, M. Farahani, M. Farhang, Novel study on keyhole less friction stir spot welding of Al 2024 reinforced with alumina nanopowder, *Int. J. Adv. Manuf. Technol.* 101 (2018) 3093–3106.
- M. Farahani, I. Sattari-Far, D. Akbari, R. Alderliesten, Numerical and experimental investigations of effects of residual stresses on crack behavior in Aluminum 6082-T6, *Proc. Inst. Mech. Eng., Part C* 226 (2012) 2178–2191.
- P. Ghabezi, M. Farahani, Characterization of cohesive model and bridging laws in mode I and II fracture in nano composite laminates, *J. Mech. Eng. Sci.* 12 (2018) 4329–4355.